

# Numerical investigation on NACA0012 airfoil with tubercular structure

Halil Hakan Açıkkel<sup>1,\*</sup>, Melike Tosun<sup>1</sup>, Mustafa Serdar Genç<sup>1</sup>, Kemal Koca<sup>1</sup>

<sup>1</sup>Wind Engineering and Aerodynamic Research Center, Department of Energy Systems Engineering, Erciyes University, KAYSERİ, TURKEY

**Abstract.** Humpback whales have very special fins, which reduce the friction force by the projections on the fins and enhance the lift force with increasing angle of attack. Thus, it has opportunity to move with less energy. In this study, the tubular structure was formed and adapted to the NACA0012 airfoil profile. Numerical modelling of tubercle wing was performed in ANSYS FLUENT. In numerical modelling,  $k-\omega$  SST and Transition SST turbulence models were used to investigate tubercle wing performance. The tubercle structure on the wing provided to canalize the flow in the tubercle cavities, thus flow separation decreased. Consequently, it was observed that the aerodynamic performance of the wing increased when the sinusoidal protrusions known as tubercle structure were applied to the leading edge of the wing.

## 1 Introduction

All living creatures in nature have optimized their systems in close familiarity to perfection, depending on their living conditions and ecosystems. People inspired these systems tried to find solutions to their problems by imitating nature and living things. Recently, many different wing structures have been obtained in the leading edge region of wing inspired by the fin structure of the humpback whales. These structures, which are affected by the morphology of humpback whales, are referred to as "tubercle structure". The aerodynamic properties of the modified tubercle wing were investigated in the wind tunnel and compared with the rigid NACA 0020 [1]. The lift and drag coefficients of the modified wing profile were measured experimentally in a water tunnel and compared with the NACA 63(4)421 [2]. Pedro and Kobayashi [3] were studied two different aerofoils and modified tubular structure wing at low Reynolds number both experimentally and numerically. Yao et al. [4] were examined aerodynamic performance of aerofoil by using numerical methods. They investigated the effects of angle of attack on aerodynamic coefficients and surface pressure. Rostamzadeh et al. [5] were done a numerical study to investigate flow over leading edge tubercle airfoil at high and low Reynolds (Re) numbers. The numerical analyzes were performed by using computational fluid dynamics at  $Re=120000$  and  $1500000$ . In these analyzes, it was aimed to see the effects of Re number on tubercle wing. Şahin and Acır [6] examined NACA0015 airfoil performance both experimentally and numerically. In numerical simulation, Spalart Almaras and  $k-\epsilon$  models was used to compare airfoil performance with experimental results. The experimental results had a good agreement with Spalart Almaras turbulence model.

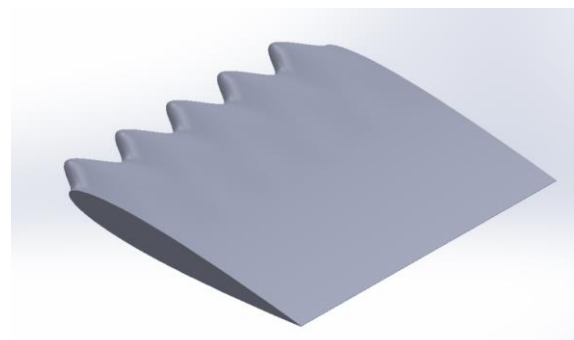
A numerical study of leading edge tubercles at low and high Reynolds numbers was done by Gawad [7]. Another experimental analysis of the tubercle wings with an aspect ratio of 4 with the Re number range between 700,000 to 3,000,000 was performed by Rocha et.al. [8].

In this study, tubercle structure design inspired by the fin of the humpback whale was made to the leading edge by using the wing profile of NACA0012.

## 2 Numerical Modelling

In the design, which is shown in Figure 1a and Figure 1b, the chord length is 0.1 m based on the NACA-0012 profile. The new design of aerofoil's span is divided into five tubercle structures. The tubercles amplitude is 0.1 chord length ( $c_t$ ). The half wave length ( $\lambda$ ) is 0.011 m. Operating Reynolds number is  $1.36 \times 10^5$  in this study.

a)



\* Corresponding author: [hhacikel@erciyes.edu.tr](mailto:hhacikel@erciyes.edu.tr)

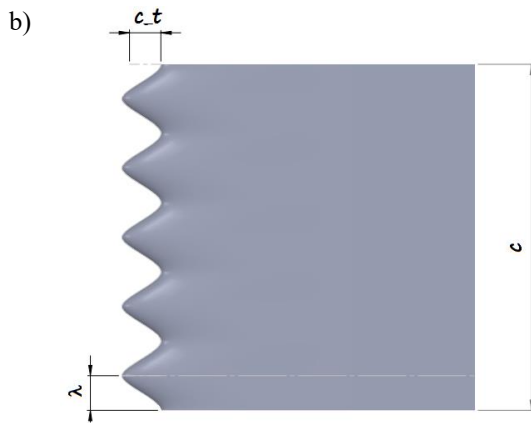


**Fig. 1.** The design of aerofoil.

Figure 2 represents the mesh structure of the flow domain. The flow domain was extended to  $20c$  towards the trailing edge of the airfoil and  $10c$  in other directions. The  $y^+$  value is lower than 1 in these numerical simulations. The  $k-\omega$  SST and Transition SST turbulence models were utilized for numerical calculations. The solution algorithm was selected SIMPLE, and momentum and turbulence kinetic energy solution methods were selected as Second Order Upwind method.

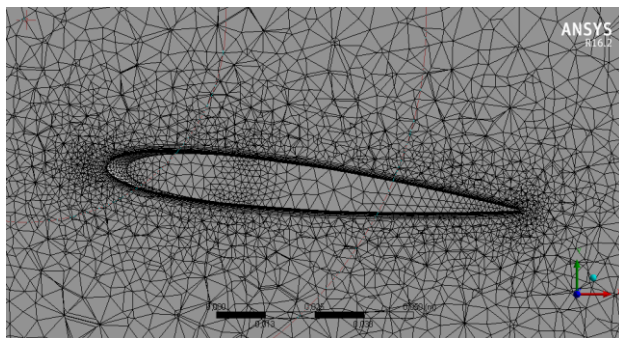


**Fig. 2.** The mesh structure of the wing.

### 2.1 Grid independence study

The grid independence study was conducted to determine mesh independence for numerical simulations which was shown in Table 1. The table gives information about mesh number and aerodynamic force coefficients. According to the results obtained from numerical analysis, 4.6 million meshes were selected for numerical solutions.

**Table 1.** Grid independence study

Mesh number	$C_L$	$C_D$
2006584	1.97399e-01	2.78839e-02
3232490	1.97678e-01	2.80084e-02
4673533	1.97678e-01	2.80084e-02

## 3 Results

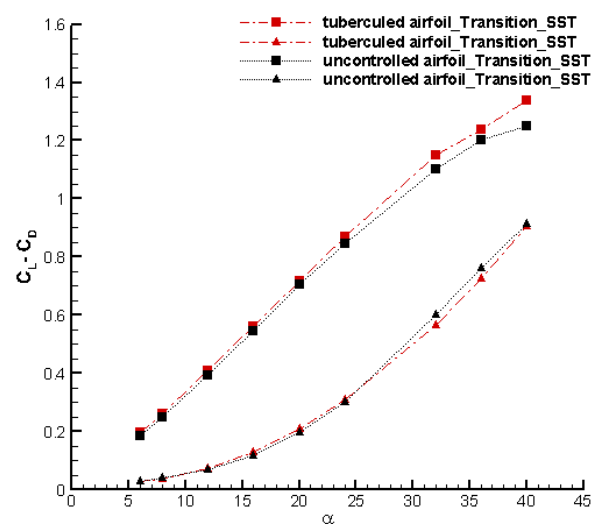
### 3.1. Aerodynamic Coefficients

Non-dimensional aerodynamic coefficients such as lift and drag coefficients were used to investigate aerodynamic performance of the wing. These coefficients are expressed in follow respectively.

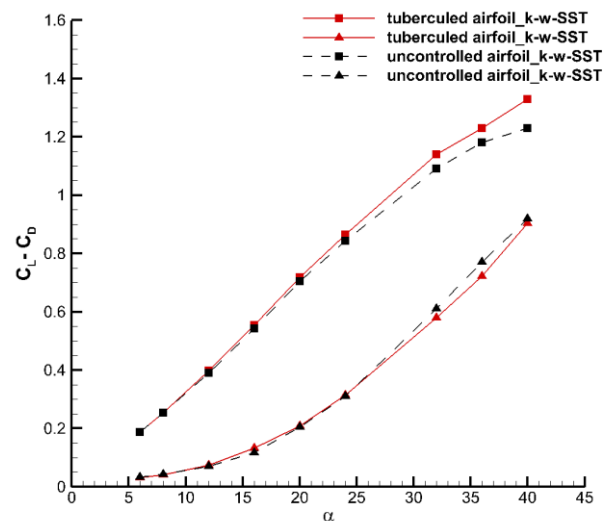
$$C_L = [(2L)] / ((\rho V^2 A)) \quad (1)$$

$$C_D = [(2D)] / ((\rho V^2 A)) \quad (2)$$

In these equations,  $\rho$  is air density,  $V$  is free stream velocity,  $A$  is area and  $L$  and  $D$  are forces.



**Fig. 3.** Aerodynamic for coefficients for the Transition SST turbulence model.



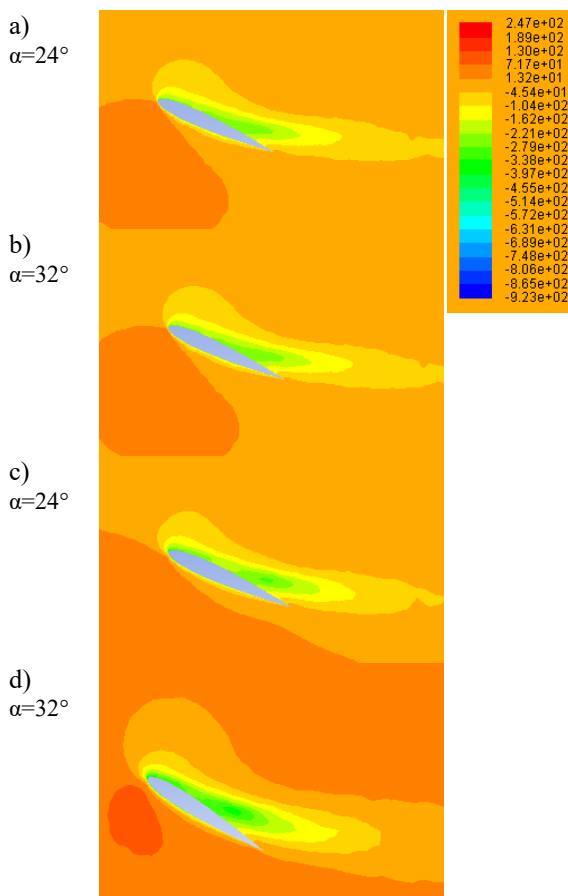
**Fig. 4.** Aerodynamic for coefficients for the  $k-\omega$  SST turbulence model.

Fig. 3 shows aerodynamic force coefficients for tubercle and rigid wings at different angles of attack. In

lower angles of attack, tubercle and uncontrolled wings presented similar performance as seen from two figures. As the angle of attack increased, the tubercled wings had a good aerodynamic performance, which meant the lift coefficient increased and the drag coefficient decreased. At angles of attack between 25°-40°, the lift coefficient was increased by using tubercle structures, and the drag coefficient was decreased slightly. Due to the fact that both turbulence models presented similar performance, flow characteristics results on the tubercled and clean wing were given for Transition SST turbulence model. Transition SST turbulence model is a transition model which is a successful model on low Re number flows [9-13].

### 3.2 Velocity Distributions

The velocity distributions give information about flow characteristics over airfoil. The velocity contours on the clean and tubercled wings airfoils at  $\alpha=24^\circ$  and  $\alpha=32^\circ$  in Transition SST model was presented in Figure 5. At these angles of attack, the tubercle gaps canalized the flow and using the tubercle structure helped the flow control.



**Fig. 5.** The velocity contours over the wings in the middle plane at  $\alpha=24^\circ$  and  $\alpha=32^\circ$  with Transition SST model for rigid wing (a-b) and for tubercle wing (c-d).

The velocity contours at cross plane of the wings presented in Figure 6. The separated flow and growing with the increasing of the angle of attack over the clean wing was showed in Figure 6 as the blue region at the rear of the wing. The tubercle structure on the wing provided to canalize the flow in the tubercle cavities, thus flow separation decreased.

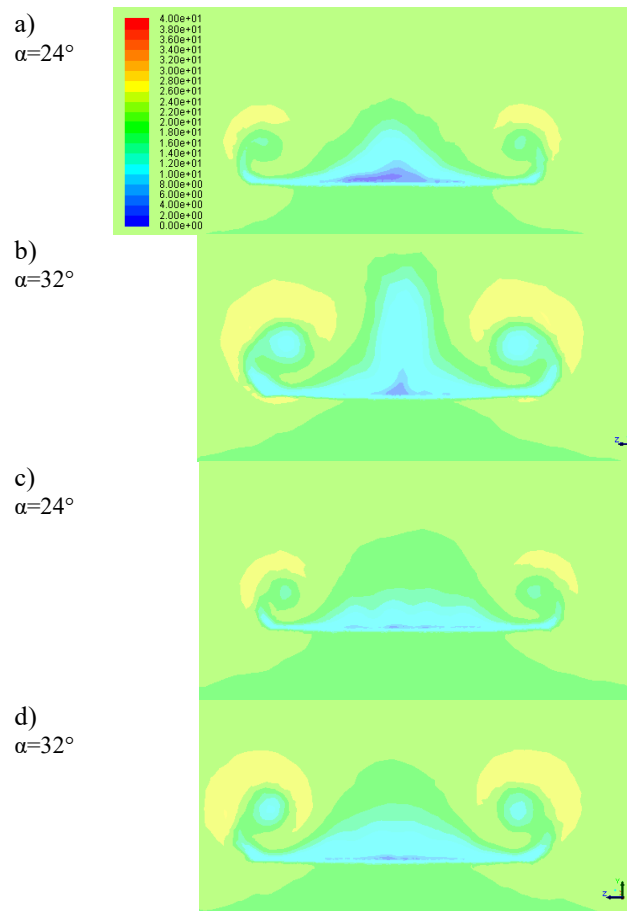


**Fig. 6.** The velocity contours at cross plane of the wings at  $\alpha=24^\circ$  and  $\alpha=32^\circ$  with Transition SST model for rigid wing (a-b) and for tubercle wing (c-d).

### 3.3 Turbulence Kinetic Energy

The turbulence kinetic energy shows the transition from laminar to turbulence and flow separation over the airfoil/wing. The turbulence kinetic energy distributions on the clean and tubercled wings airfoils at  $\alpha=24^\circ$  and  $\alpha=32^\circ$  in Transition SST model was given in Figure 7. The flow on the clean wing separated from the trailing edge of the wing and the flow separation enlarged with the increasing of the angle of attack. Utilizing the tubercle structure on the wing provided to trigger the transition. The flow over the wing become the turbulent flow and gained a resistance to flow separation. The canalized flow with the tubercled structure supplied the flow control.

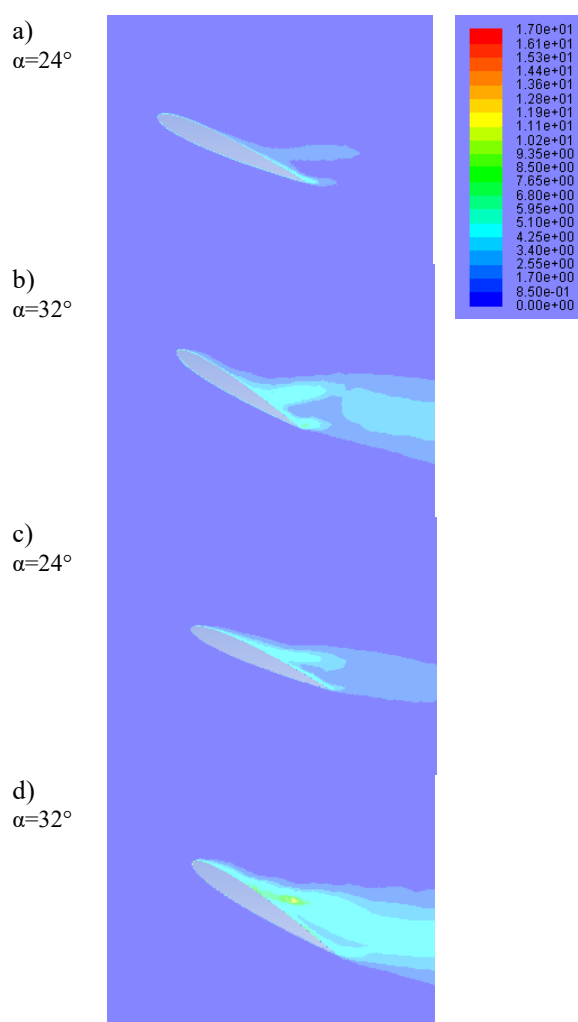


**Fig. 7.** The turbulence kinetic energy contours over the wings in the middle plane at  $\alpha=24^\circ$  and  $\alpha=32^\circ$  with Transition SST model for rigid wing (a-b) and for tubercle wing (c-d).

## 4 Conclusion

In this study, the tubercle structure adapted to the NACA0012 airfoil profile was investigated numerically. Numerical modelling of tubercle wing was carried out in ANSYS FLUENT using  $k-\omega$  SST and Transition SST turbulence models. The tubercle structure on the wing provided to canalize the flow in the tubercle cavities, thus flow separation decreased. Utilizing the tubercle structure on the wing provided to trigger the transition. The flow over the wing become the turbulent flow and gained a resistance to flow separation. The canalized flow with the tubercled structure supplied the flow control. Consequently, the aerodynamic performance of the wing increased when the tubercle sinusoidal protrusions were applied to the wing.

## References

1. Miklosovic, D. S., Murray, M. M., Howle, L. E., & Fish, F. E. *Physics of fluids* 16.5 (2004): L39-L42.
2. Johari, H., Henoeh, C. W., Custodio, D., & Levshin, A. *AIAA journal* 45.11 (2007): 2634-2642.

3. Carreira Pedro, Hugo, and Marcelo Kobayashi. 46th AIAA aerospace sciences meeting and exhibit. 2008.
4. Yao, Ji, et al. *Procedia Engineering* 31 (2012): 80-86.
5. Rostamzadeh, Nikan, Richard M. Kelso, and Bassam Dally. *Theoretical and Computational Fluid Dynamics* 31.1 (2017): 1-32.
6. Şahin, İzzet, and Adem Acir. *International Journal of Materials, Mechanics and Manufacturing* 3.1 (2015): 22-25.
7. Gawad, Ahmed Farouk Abdel. *International Mechnaical Engineering Congresss & Exposition*. 2012.
8. Rocha, F. A., de Paula, A. A., Sousa, M. D., Cavalieri, A. V., & Kleine, V. G. (2018). 2018 Applied Aerodynamics Conference (p. 3816).
9. M.S. Genç, U. Kaynak, H. Yapıcı, *European Journal of Mechanics B/Fluids*, 30(2) 218-235 (2011).
10. M.S. Genç, *Proc IMechE, Part C- Journal of Mechanical Engineering Science*, Vol 224 (10), pp. 2155 – 2164, 2010.
11. I. Karasu, M. Özden, M.S. Genç, *Journal of Fluids Engineering-Transactions of The ASME*, 140(12) 121102-1-121102-15 (2018).
12. H. Demir, M. Özden, M.S. Genç, M. Çağdaş. In *EPJ Web of Conferences* (Vol. 114, p. 02016). EDP Sciences, (2016)
13. M.S. Genç, K. Koca, H.H. Açikel. *Energy*, 176, 320-334 (2019)